

Noisy multistate voter model for flocking in finite dimensions

Ernesto S. Loscar and Gabriel Baglietto

*Instituto de Física de Líquidos y Sistemas Biológicos (IFLYSIB), UNLP, CCT La Plata–CONICET,
Calle 59 no. 789, B1900BTE La Plata, Argentina*

Federico Vazquez*

Instituto de Cálculo, FCEN, Universidad de Buenos Aires and CONICET, C1428EGA Buenos Aires, Argentina

(Received 26 January 2021; accepted 25 August 2021; published 8 September 2021)

We study a model for the collective behavior of self-propelled particles subject to pairwise copying interactions and noise. Particles move at a constant speed v on a two-dimensional space and, in a single step of the dynamics, each particle adopts the direction of motion of a randomly chosen neighboring particle within a distance $R = 1$, with the addition of a perturbation of amplitude η (noise). We investigate how the global level of particles' alignment (order) is affected by their motion and the noise amplitude η . In the static case scenario $v = 0$ where particles are fixed at the sites of a square lattice and interact with their first neighbors, we find that for any noise $\eta > 0$ the system reaches a steady state of complete disorder in the thermodynamic limit, while for $\eta = 0$ full order is eventually achieved for a system with any number of particles N . Therefore, the model displays a transition at zero noise when particles are static, and thus there are no ordered steady states for a finite noise ($\eta > 0$). We show that the finite-size transition noise vanishes with N as $\eta_c^{1D} \sim N^{-1}$ and $\eta_c^{2D} \sim (N \ln N)^{-1/2}$ in one- and two-dimensional lattices, respectively, which is linked to known results on the behavior of a type of noisy voter model for catalytic reactions. When particles are allowed to move in the space at a finite speed $v > 0$, an ordered phase emerges, characterized by a fraction of particles moving in a similar direction. The system exhibits an order-disorder phase transition at a noise amplitude $\eta_c > 0$ that is proportional to v , and that scales approximately as $\eta_c \sim v(-\ln v)^{-1/2}$ for $v \ll 1$. These results show that the motion of particles is able to sustain a state of global order in a system with voter-like interactions.

DOI: [10.1103/PhysRevE.104.034111](https://doi.org/10.1103/PhysRevE.104.034111)**I. INTRODUCTION**

The study of the collective properties of systems composed by self-propelled individuals has been the focus of intense research in the last two decades [1–3]. The flocking behavior of a large group of animals is observed in many different species such as fish, birds, bacteria, and insects, among others. From a statistical physics viewpoint, the interactions between particles in a system are responsible of its collective behavior, and lead to well-characterized classes represented by archetype models. For the case of flocking, the alignment interaction among individuals is usually modeled as a local averaging of moving directions of nearby individuals, plus a noise that accounts for errors in the average process [4]. A crucial role in the emergent behavior of the system is played by the displacement of the individuals, which changes dramatically its ordering properties [5].

Within the context of flocking, the dynamics of collective alignment in groups of fish was recently studied in [6]. The authors performed experiments with cichlid fish *Etoplus suratensis* that swim in a circular shallow tank, in order to explore how schooling is affected by the fish group size. The level of group alignment is quantified by a vector order parameter \mathbf{M} that is the average velocity of fish, also called group

polarization, in such a way that $|\mathbf{M}| \sim 1$ corresponds to a polarized state where fish move in a coherent direction, while $|\mathbf{M}| \sim 0$ represents a collectively disordered state—each fish moving in a random direction. Performing the experiments for group sizes $N = 15, 30$, and 60 , they found that the collective alignment $|\mathbf{M}|$ increases as N decreases. An insight into this phenomenon is given by a phenomenological stochastic differential equation (SDE) for the time evolution of \mathbf{M} , where its parameters were extracted from the experimental data. It is shown that group polarization is the result of the interplay between the drift and the demographic (population) noise terms in the SDE, that is, the fewer the fish, the greater the demographic noise and so the greater the alignment level. Thus, they conclude that schooling (highly polarized and coherent motion) is induced by the intrinsic population noise that arises from the stochasticity related to the finite number of interacting fish. They derived the SDE for \mathbf{M} by means of a mean-field (MF) model in which particles (fish) interact by pairs and follow a simple imitation dynamics: each particle either copies the direction of another random particle or spontaneously changes its direction, modeled as an external noise of amplitude η . They also show that other ternary or higher-order aligning interactions, including local averages like in the Vicsek-like family of models, are unnecessary to explain these experimental results. Therefore, they arrive to the conclusion that the minimal theoretical mechanism that reproduces the collective alignment properties of fish observed

*fedevazmin@gmail.com

in the experiments is that of pairwise interactions with copying dynamics and noise. We notice that the noiseless version of this particular alignment dynamics that induces flocking was first introduced in [7], where the authors study the collective motion of particles on a two-dimensional (2D) space subject to voter-like interactions, that is, each particle aligns its direction of motion with that of a random neighboring particle within an interaction radius.

From the theoretical point of view, an interesting result can be inferred from the work in [6] by analyzing the SDE for the group polarization \mathbf{M} . That is, this equation predicts complete order ($|\mathbf{M}| = 1$) for zero noise ($\eta = 0$) and full disorder ($|\mathbf{M}| = 0$) for any finite noise amplitude $\eta > 0$ in the $N \rightarrow \infty$ limit. This observation is in agreement with recent analytical results obtained in a similar model with a discrete set of S angular directions, a multistate voter model (MSVM) with external noise [8], where it is shown that the order parameter $|\mathbf{M}|^2$ approaches 1.0 as $1 - |\mathbf{M}|^2 \sim \eta^2 N$ in the $\eta \rightarrow 0$ limit, and vanishes when N increases as $1/(\eta^2 N)$ for any $0 < \eta \ll 1$. Thus, the partial order obtained with voter interactions and noise in a MF setup is only a finite size effect that eventually disappears in the thermodynamic limit. These results suggest a peculiar order-disorder transition at zero noise, unseen in related flocking models such as the binary Vicsek model [9] where each particle averages its direction with that of other random particle, and the transition happens at a critical noise larger than zero. However, we notice that the experimental results obtained in [6] correspond to fish moving on a 2D setup (tank), while both the SDE and the model in [8] are for a MF setup (infinite dimension), where every particle interacts with any other particle, and thus motion plays no role in the dynamics. It is natural, therefore, to wonder whether these results hold when particles move on a 2D space. Do space and motion affect the transition at zero noise?

In this article we study a noisy multistate voter model for flocking in finite dimensions, and we investigate the order-disorder phase transition in different case scenarios. We start by analyzing the simplest case of all-to-all interactions or MF. We then explore the static case where each particle occupies a site of a square lattice and interacts with its first nearest-neighbors, and we finally study the dynamic case in which particles move on a 2D continuous space and change their direction when they interact with other nearby particles that are located within a distance $R = 1$. In the case that particles are allowed to have only two possible angular states and interact on a MF setup, the model turns to be equivalent to the noisy voter model (NVM) introduced in [10,11], in which each individual of a population holds one of two states (opinions) that are updated by either copying the state of a random neighbor or spontaneously switching state (noise). In the absence of noise, any finite population eventually reaches full order (consensus) in all dimensions, as in the original voter model [12,13], with all individuals sharing the same opinion. However, the addition of a weak noise leads to a bistable regime in which the system jumps between two steady states corresponding to a quasiconsensus in one or the other opinion [10,11], while for strong noise the system remains disordered. This is in line with the fact that adding thermal bulk noise in the voter model destroys global order in any dimension [14], even when the noise is

weak. In square lattices, the NVM is equivalent to a particular limit of the catalytic reaction model with desorption originally introduced in [15] and widely studied subsequently [16,17], which exhibits a finite-size transition induced by noise called *saturation* transition [18–20]. More recently, the dynamics of the NVM has been investigated in complex networks [21–23], and its version with multiple states has been explored in fully connected systems [8,24]. Also, an asymmetric variant of the NVM with long-range interactions has recently been proposed to study the competition between two species for territory [25].

While in 2D lattice models bulk noise inhibits the formation of long-range order in the thermodynamic limit, it is known that in flocking systems the displacement of particles plays an ordering role. This ordering phenomenon is observed in the Vicsek model, thought as a nonequilibrium version of the XY model in two dimensions with particles moving ballistically in the directions of their spins. That is, while the Vicsek model can sustain long-range order for finite values of noise amplitude due to particles' motion [5], the 2D XY model is unable to do so [26]. Then, the velocity of particles in Vicsek-type models leads to steady states associated with a new ordered phase below a transition noise η_c . However, voter-type interactions (copying) are different from Vicsek-type interactions (averaging), leading to different behaviors in MF and three dimensions: long-range order in the XY model, and disorder in the NVM. Therefore, in the flocking voter model (FVM) studied in this article, we expect a nontrivial competition between the ordering mechanism generated by particles' motion and the typical disordering effect induced by noisy voter interactions that leads to complete disorder in the thermodynamic limit. Thus, we aim to explore whether the ordered phase observed in flocking models is still present in the FVM, or it is rather completely suppressed by noise.

The rest of the article is organized as follows. In Sec. II we define the model. Section III presents MF results, while Sec. IV is dedicated to the static version of the model in one-dimensional (1D) and 2D square lattices. In Sec. V we study the dynamic version of the model in a continuous 2D space. We investigate the effects of particles' velocity in the transition, with a particular focus on the behavior at low speeds in the thermodynamic limit. Finally, in Sec. VI we summarize and give some conclusions.

II. THE MODEL

A set of N particles are allowed to move at a constant speed v on a 2D square box of side L with periodic boundary conditions. The position and velocity of particle i ($i = 1, 2, \dots, N$) at time t are denoted by $\mathbf{r}_i^t = (x_i^t, y_i^t)$ and $\mathbf{v}_i^t = (v \cos \theta_i^t, v \sin \theta_i^t)$, respectively, where $v = |\mathbf{v}_i^t|$ is the particle's speed and θ_i^t is its angular moving direction. The density of particles $\rho = N/L^2$ is fixed at 0.5 in our analysis, unless stated. Initially, each particle adopts a random position inside the box and points in a random direction. In a given time step $\Delta t = 1$ of the dynamics, each particle i updates its position and direction according to

$$\mathbf{r}_i^{t+1} = \mathbf{r}_i^t + \mathbf{v}_i^t \Delta t, \quad (1a)$$

$$\theta_i^{t+1} = \theta_j^t + \xi_i^{t+1}, \quad (1b)$$

where θ_j^t is the moving direction of a randomly chosen particle j that is inside a disk of radius $R = 1$ centered at \mathbf{r}_i^t , and ξ_i^t is a random angle drawn uniformly in $[-\eta\pi, \eta\pi)$ with amplitude η ($0 < \eta < 1$). This update is performed for all particles at the same time (parallel update). That is, each particle moves at a constant speed v following a given straight path and updates its direction at integer times $t = 1, 2, 3, \dots$, by adopting the direction of a random neighboring particle with an error of amplitude η . If a particle has no neighbors inside its interaction range R , then its direction is changed only by the noise ξ .

In flocking models, noise—in its various forms—plays a fundamental role in the behavior of the system. It is known that the amplitude of noise η induces an order-disorder phase transition, from a phase where a large fraction of particles move in a similar direction (order) for small η , to a phase in which particles move in random directions (disorder) for large η . To study this phenomenon in the FVM we define the order parameter (see, for instance, [6,7])

$$\varphi(t) \equiv \frac{1}{vN} \left| \sum_{i=1}^N \mathbf{v}_i^t \right| = \frac{1}{N} \sqrt{\left[\sum_{i=1}^N \cos \theta_i^t \right]^2 + \left[\sum_{i=1}^N \sin \theta_i^t \right]^2} \quad (2)$$

that measures the level of collective alignment in the system (magnitude of the normalized mean velocity of all particles), and the susceptibility

$$\chi \equiv N[\langle \varphi^2 \rangle - \langle \varphi \rangle^2], \quad (3)$$

which accounts for the amplitude of fluctuations of φ at the stationary state. Here $\langle \varphi^m \rangle$ is the m th moment of φ , and the symbol $\langle \cdot \rangle$ represents the average value of a given magnitude over many realizations of the dynamics at the steady state.

Our aim is to explore via computational simulations and scaling theory how space and motion affects the phase transition in the FVM. For that, we first study the model in MF ($R = L$), we then explore the static case $v = 0$ in lattices, and we finally investigate the dynamic case $v > 0$ in two dimensions.

III. MEAN FIELD

In order to gain an insight into the behavior of the FVM, we start by analyzing in this section the simplest case scenario of all-to-all interactions or MF, which corresponds to the large interaction range limit $R \rightarrow L$ of the model defined in Sec. II. In this case, the dynamics of the angular directions of particles θ is independent of the positions of particles, and thus it is entirely determined by Eq. (1b). That is, each particle simply adopts the direction of another randomly chosen particle in the system, with the addition of noise. This dynamics is equivalent to that of the multistate voter model with imperfect copying introduced and studied in [8], in the limit of continuum angular states. In a single time step $\Delta t = 1/N$, a particle i with state θ_i is picked at random, then it copies the state θ_j of another randomly chosen particle j , and this state is slightly perturbed:

$$\theta_i(t + \Delta t) = \theta_j(t) + \xi_i(t + \Delta t). \quad (4)$$

We note that we are implementing here a *random update* (also called *sequential update*), in which one random particle updates its state in a time step, unlike the *parallel update* where all N particles are updated at once. However, we have verified that the behavior of the macroscopic variables φ and χ under the parallel update is recovered by making the substitution $N \rightarrow 2N$ in the results obtained with the random update, as mathematically proved by Blythe and McKane [27] for population genetic models akin to the voter model. Inversely, the transformation $N \rightarrow N/2$ allows us to obtain the behavior under the random update from the results with parallel update. Implementing a random update allows a direct comparison of the simulation results in MF with the theoretical results obtained in [8].

Figure 1 shows simulation results for the model in MF. Data points correspond to average values in a time interval after the system reached the stationary state, between times $t = 10^6$ and $t = 2 \times 10^7$, and over 10 independent realizations. In Fig. 1(a) we observe that the order parameter φ continuously decreases as η increases, and that approaches the value $\varphi = 1$ (full order) as $\eta \rightarrow 0$, which corresponds to the absorbing consensus state obtained in the zero noise case $\eta = 0$, as is known from previous works of the multistate voter model [7,8,28,29]. We also see that, for a fixed value of $\eta > 0$, φ vanishes as the system size N increases, suggesting that $\varphi \rightarrow 0$ for any $\eta > 0$ in the $N \rightarrow \infty$ limit. Indeed, an expression for the scaling of $\langle \varphi \rangle$ with η and N that confirms this assumption can be obtained from analytical results of this model recently presented in [8], for an order parameter $\psi = \varphi^2$. It was shown in [8] that $\langle \psi \rangle \sim (\eta^2 N)^{-1}$ for $\eta \ll 1$ and $\eta^2 N \gtrsim 1$, and thus assuming $\langle \varphi \rangle \sim \langle \psi \rangle^{1/2}$ we obtain the approximate MF behavior

$$\langle \varphi \rangle_{\text{MF}} \sim (\eta^2 N)^{-1/2} \quad \text{for } \eta \ll 1 \text{ and } \eta^2 N \gtrsim 1. \quad (5)$$

In the inset of Fig. 1(a) we plot the data as a function of the scaling variable $x_{\text{MF}} \equiv \eta^2 N$, where we can see that $\langle \varphi \rangle_{\text{MF}}$ obeys the power-law decay from Eq. (5) for $\eta^2 N \gtrsim 1$ (dashed line). We also observe a good collapse of the curves for different system sizes in the entire range of x_{MF} , showing that the order parameter is a function of x_{MF} , $\langle \varphi \rangle_{\text{MF}} = f(\eta^2 N)$, with $f(x_{\text{MF}}) \sim x_{\text{MF}}^{-1/2}$ for $x_{\text{MF}} \gtrsim 1$.

The results above imply that in the absence of noise $\eta = 0$ the system reaches full order ($\varphi = 1$), but a tiny amount of noise $\eta > 0$ is enough to drive the system to complete disorder ($\varphi = 0$) in the thermodynamic limit, which suggests a transition at zero noise. To study this in more detail, we show in Fig. 1(b) the behavior of the susceptibility χ with η . We observe that the curve for a given system size N exhibits a maximum that is an indication of a transition that depends on N , between an ordered phase for $\eta < \eta_c(N)$ and a disordered phase for $\eta > \eta_c(N)$, where the transition point $\eta_c(N)$ is estimated as the location of the peak. In Fig. 2(a) we plot the transition noise η_c vs N (circles), where we can see that η_c vanishes as N increases following a power-law behavior $N^{-\alpha}$, with a best fitting exponent $\alpha = 0.5 \pm 0.015$. This implies a transition value $\eta_c(\infty) = 0$ in the thermodynamic limit. In Fig. 2(b) we see that the maximum value of the susceptibility increases with N as $\chi^{\text{max}} \sim N^\gamma$, where $\gamma \simeq 1.01 \pm 0.01$ is the best fitting exponent.

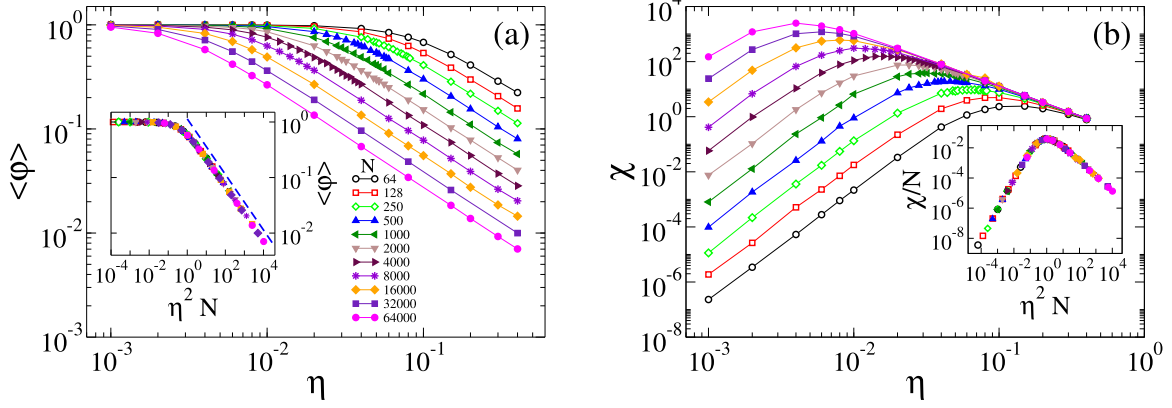


FIG. 1. Results of the FVM in MF. (a) Average value of the order parameter ϕ at the stationary state as a function of noise amplitude η for the system sizes N indicated in the legend. Inset: Collapse of the data points when they are plotted as a function of the scaling variable $x_{MF} = \eta^2 N$. The dashed line has slope $-1/2$. (b) Susceptibility χ vs η for the same system sizes as in panel (a). Inset: Collapse of the data when it is plotted vs x_{MF} and the y-axis is rescaled by N^{-1} . Averages were done in a time window $\Delta t \sim 10^7$ over 10 independent realizations.

These scalings can be nicely verified by assuming that χ is also a function of the scaling variable $x_{MF} = \eta^2 N$ for ϕ in Fig. 1. Indeed, rescaling the y-axis of Fig. 1(b) by N^{-1} and plotting the resulting data vs x_{MF} we find a good collapse of all curves for different N values (see inset), showing that the MF susceptibility behaves as

$$\chi_{MF} = Ng(\eta^2 N), \quad (6)$$

where $g(x_{MF})$ is a smooth function of x_{MF} . From Eq. (6) we have that at the MF transition point η_c^{MF} is $\chi_{MF}^{\max}/N = g[(\eta_c^{MF})^2 N] = \text{constant}$ and, therefore,

$$\eta_c^{MF} \sim N^{-1/2}, \quad (7)$$

in agreement with numerical results [Fig. 2(a)].

In summary, the mean-field version of the FVM exhibits an order-disorder phase transition at zero noise $\eta_c = 0$ in

the thermodynamic limit, between a perfectly ordered phase where $\phi = 1$ for $\eta = 0$ and a completely disordered phase where $\phi = 0$ for $\eta > 0$.

IV. STATIC CASE $v = 0$ IN ONE AND TWO DIMENSIONS

In this section we analyze the static version of the FVM in finite dimensions. For that, we consider that each particle occupies a site of a square lattice of length L and d dimensions ($N = L^d$ sites), and interacts with its 2^d nearest neighbors only. We have simulated the dynamics of the model under the random update described in Sec. III on lattices of dimensions $d = 1$ and $d = 2$ with periodic boundary conditions. In a time step $\Delta t = 1/N$, a randomly selected particle copies the angular state of a first neighbor chosen at random, with the addition of an error of amplitude η . Implementing a random

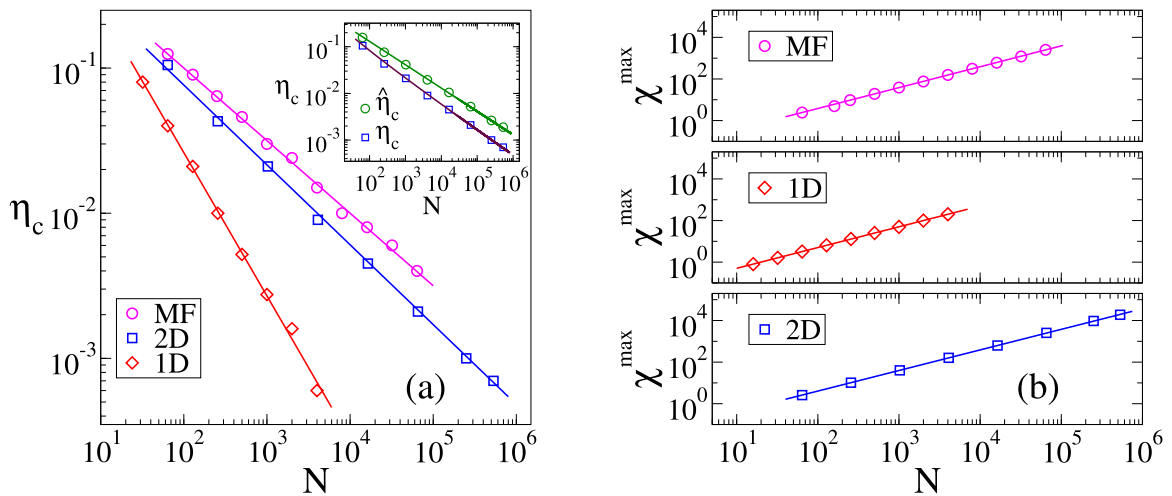


FIG. 2. Results of the FVM in MF (circles) and in square lattices of dimensions $d = 1$ (diamonds) and $d = 2$ (squares). (a) Transition noise η_c vs system size N . Straight lines are best power-law fits $\eta_c = AN^{-\alpha}$ with exponents $\alpha = 0.5 \pm 0.015$ (MF), 0.99 ± 0.02 ($d = 1$) and 0.56 ± 0.01 ($d = 2$). Inset: η_c for $d = 2$ (squares) and the effective noise $\hat{\eta}_c = \eta_c \sqrt{-\ln \eta_c}$ (circles). The upper solid line is the best power-law fit $\hat{\eta}_c \simeq BN^{-1/2}$, with $B = 1.3 \pm 0.04$, while the bottom solid curve is the approximation $\eta_c \simeq 1.8(N \ln N)^{-1/2}$ from Eq. (15c). (b) Maximum value of the susceptibility χ^{\max} vs N . Best power-law fits $\chi^{\max} \sim N^\gamma$ (straight lines) have exponents $\gamma = 1.01 \pm 0.01$ (MF), 0.997 ± 0.005 ($d = 1$) and 0.99 ± 0.01 ($d = 2$).

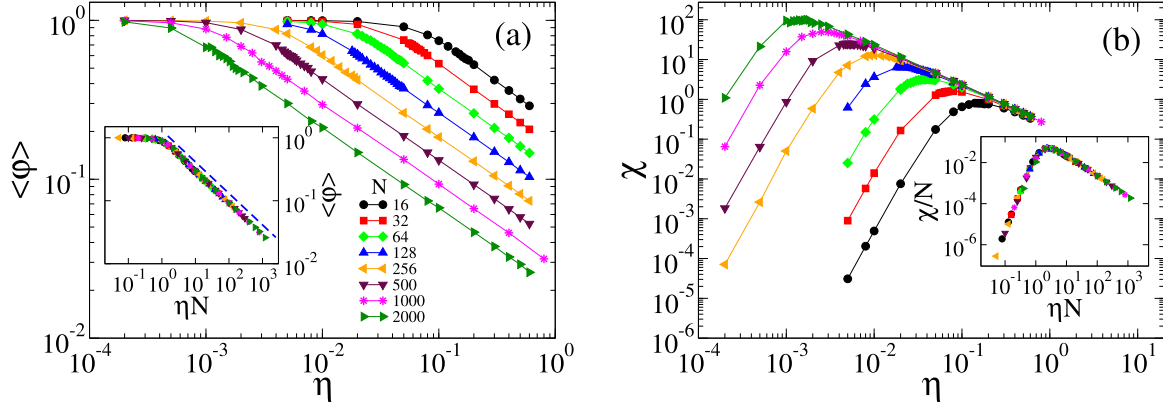


FIG. 3. Results of the static version of the FVM in one dimension. (a) Average value of ϕ at the stationary state vs η for the system sizes N indicated in the legend. Inset: Same data vs the scaling variable $x_{1D} = \eta N$ showing the collapse of curves for different N values. The dashed line has slope $-1/2$. (b) Susceptibility χ vs η for the same system sizes as in panel (a). Inset: x - and y -axis are rescaled by N and N^{-1} , respectively, to show the collapse of the data.

update allows a direct comparison with known numerical and analytical results of the two-state VM on lattices (see below), and provides the analytical background to obtain the scalings of ϕ and χ for the MSVM. We have run simulations and verified that the behavior of ϕ and χ , and the scaling of η_c under the parallel update are the same as those obtained for the random update after the system size rescaling $N \rightarrow N/2$, as happens in MF (Sec. III).

Figure 3 shows simulation results for the FVM in one dimension. The behavior of $\langle\phi\rangle$ and χ are similar to those of the MF model, with a scaling variable $x_{1D} \equiv \eta N$ in this 1D case. The variable x_{1D} was obtained from the behavior of the transition noise η_c^{1D} with N given by the peak of χ in Fig. 3(b). We found $\eta_c^{1D} \sim N^{-\alpha}$, with $\alpha = 0.99 \pm 0.02$ [Fig. 2(a)], while for the peak of the susceptibility we found the scaling $\chi^{\max} \sim N^\gamma$, with $\gamma = 0.997 \pm 0.005$ [Fig. 2(b)]. Therefore, assuming the scalings

$$\eta_c^{1D} \sim N^{-1} \quad \text{and} \quad (8)$$

$$\chi^{\max} \sim N, \quad (9)$$

we arrive at the following scaling for the susceptibility:

$$\chi_{1D} = N g_1(\eta N), \quad (10)$$

and thus the scaling variable is $x_{1D} = \eta N$, as stated above. Indeed, we can check in the insets of Fig. 3 the collapse of the curves for different system sizes when the data are plotted vs x_{1D} , and the y -axis in Fig. 3(b) is rescaled by N^{-1} . Also, in the inset of Fig. 3(a) we show that the order parameter scales as $\langle\phi\rangle_{1D} \sim x_{1D}^{-1/2}$ for $x_{1D} \gtrsim 1$ (dashed line), which exhibits the same behavior with respect to the scaling variable as that of MF [Eq. (5)], i.e., a power-law decay with exponent $1/2$.

The scaling relation (8) shows that the transition noise vanishes with N , and, therefore, we conclude that the static version of the FVM in one dimension exhibits an order-disorder transition at zero noise in the thermodynamic limit, as happens in MF.

We repeated the same analysis for the FVM model on 2D lattices. Simulation results are presented in Fig. 4, where the data collapse was obtained by means of two different scaling

variables, as we describe below. As happens for the MF and the 1D cases, the transition noise (given by the maximum of the susceptibility) decays as a power law with the system size N as $\eta_c^{2D} \sim N^{-\alpha}$ [square symbols in Fig. 2(a)], with a best power-law fitting exponent $\alpha \simeq 0.56 \pm 0.01$. Even though this exponent is different from the MF and 1D exponents 0.5 and 1 , respectively, this numerical scaling implies an extrapolated transition noise $\eta_c^{2D} = 0$ in the $N \rightarrow \infty$ limit. The peak of the susceptibility χ^{\max} seems to increase linearly with N as in MF and 1D, with a best-fitting exponent $\gamma \simeq 0.99 \pm 0.01$ [Fig. 2(b)]. Based on these results, we plot $\langle\phi\rangle$ and χ/N as a function of $\eta^2 N^{1.1}$ in Figs. 4(a) and 4(b), respectively, where we observe a good collapse of curves for different system sizes. For the sake of simple comparison, we have also collapsed the same data using the MF scaling variable

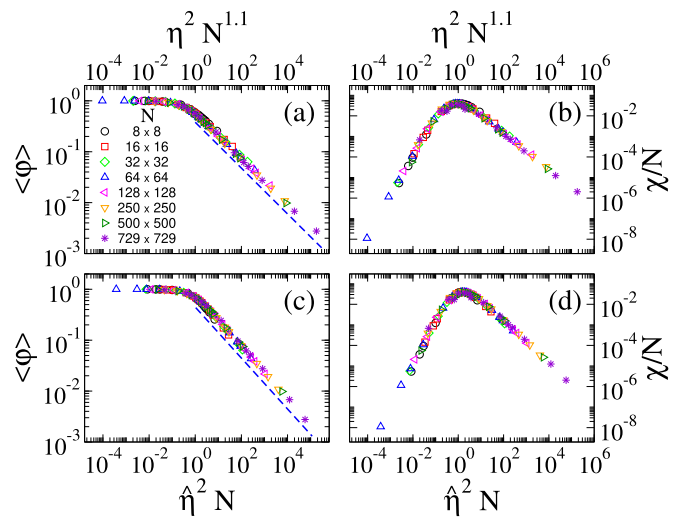


FIG. 4. Static version of the FVM in 2D lattices. (a) Average order parameter $\langle\phi\rangle$ and (b) normalized susceptibility χ/N vs the scaling variable $\eta^2 N^{1.1}$ for the system sizes N indicated in the legend. (c) $\langle\phi\rangle$ and (d) χ/N vs the scaling variable $x_{2D} = \hat{\eta}^2 N$ for the same system sizes as in panels (a) and (b), with $\hat{\eta} = \eta\sqrt{-\ln \eta}$. Dashed lines in panels (a) and (c) have slopes -0.45 and $-1/2$, respectively.

$\eta^2 N$ instead, and found that the data points do not fall into a single curve but they look rather disperse (plot not shown). Therefore, we conclude that the 2D case appears to have its own scaling variable, which is proportional to a nontrivial power of N .

A more appealing scaling variable can be obtained from known results of the behavior of the surface-reaction model introduced by Fichthorn, Gulari, and Ziff (FGZ) in [16] and studied later in [18,18–20], akin to the two-state NVM [10,11], which we believe it belongs to the same class of the MSVM for flocking studied here. In the FGZ model, N particles of two different species A and B occupy the sites of a square lattice that simulates a catalytic substrate. In a single step, two possible reaction events can take place: (1) With probability p_d one particle is chosen at random and desorbs, and the vacant site is immediately occupied with a particle of species A or B with the same probability $1/2$. This corresponds to the external noise of the NVM that switches the state of a particle with probability $p_d/2$. (2) With the complementary probability $1 - p_d$ a pair of neighboring sites is chosen at random, and, if it is an AB pair, both particles desorb and are replaced with an AA or a BB pair, equiprobably. This represents the copy dynamics of the NVM. The control parameter of the FGZ model is the desorption probability p_d (noise amplitude). The steady state at $p_d = 0$ is a poisoned absorbing state with a coverage equals to 1.0 (all particles in state A or B), which is analogous to complete order for $\eta = 0$ in the FVM. For $p_d > 0$ the coverage is smaller than 1.0, depending on the values of p_d and N , similarly to the partial order in the FVM.

It turns out that the scaling variables that we obtained for the FVM in MF and one dimension are the same as those of the FGZ model, by making a suitable change of variables. In the FGZ model they obtained analytically the scaling variables $X_{MF} = p_d N$ in MF ($d = 3$) and $X_{1D} = p_d^{1/2} N$ in one dimension [18,19], while in the FVM are $x_{MF} = \eta^2 N$ in MF and $x_{1D} = \eta N$ in one dimension. Thus, the scaling variables of both models match if we make the substitution $p_d \rightarrow \eta^2$. Finally, 2D is a marginal dimension in the FGZ model, with a scaling variable similar to that of MF with a logarithmic correction in p_d , that is, $X_{2D} = p_d \ln(1/p_d) N$. Therefore, for the FVM in two dimensions we expect a scaling variable $x_{2D} = \hat{\eta}^2 N$, where we have defined an effective noise amplitude $\hat{\eta} \equiv \eta \sqrt{-\ln \eta}$.

Figures 4(c) and 4(d) show $\langle \varphi \rangle$ and χ/N plotted as a function of the scaling variable x_{2D} , where we see a good data collapse. Even though this collapse with x_{2D} seems as good as that with $\eta^2 N^{1.1}$ [Figs. 4(a) and 4(b)], the advantage of using $x_{2D} = \hat{\eta}^2 N$ is twofold: we are not fitting any parameter and we recover the linear dependence on N found in MF and 1D scaling variables x_{MF} and x_{1D} . Additionally, Fig. 4(c) shows that the order parameter scales as $\langle \varphi \rangle_{2D} \sim x_{2D}^{-1/2}$ for $x_{2D} \gtrsim 1$ (dashed line), consistent with the power-law decay found in MF and one dimension. In comparison, $\langle \varphi \rangle_{2D}$ decays as a power law of $\eta^2 N^{1.1}$ with a nontrivial exponent -0.45 [dashed line in Fig. 4(a)]. Finally, from the scaling relation for the susceptibility

$$\chi_{2D} = N g_2(\hat{\eta}^2 N), \quad (11)$$

where g_2 is a smooth function of x_{2D} [see Fig. 4(d)], we obtain the effective transition noise

$$\hat{\eta}_c^{2D} \simeq B N^{-1/2} \quad (12)$$

in two dimensions, where B is a proportionality constant. Interestingly, the exponent $\hat{\alpha}^{2D} \equiv 1/2$ in the 2D case agrees with that of the MF case [Eq. (7)]. In the inset of Fig. 2(a) we compare the effective transition noise

$$\hat{\eta}_c^{2D} = \eta_c^{2D} \sqrt{-\ln \eta_c^{2D}} \quad (13)$$

from simulations (circles) with the approximate scaling given by Eq. (12) (upper solid line), with a best fitting constant $B = 1.3 \pm 0.04$. The good agreement between simulations and Eq. (12) shows that the transformation of the original noise η_c^{2D} into the effective noise $\hat{\eta}_c^{2D}$ leads to power-law decay in N with a MF exponent $\hat{\alpha}^{2D} = 1/2$.

We can now obtain an approximate expression for the transition noise assuming that it has the power-law behavior $\eta_c^{2D} \simeq A N^{-\alpha}$ as found numerically [squares in Fig. 2(a)], where the exponent α depends on N and $A \simeq 0.96$ is a constant obtained from the fitting of the data. Starting from the relation Eq. (13) between the effective and original noise, we apply the logarithm at both sides and replace $\ln \hat{\eta}_c^{2D}$ by $\ln B - \frac{1}{2} \ln N$ from Eq. (12) and $\ln \eta_c^{2D}$ by $\ln A - \alpha \ln N$, which leads to

$$(2\alpha - 1) \ln N - 2 \ln(A/B) - \ln(\ln N) - \ln \alpha = 0, \quad (14)$$

after doing some algebra and rearranging terms. We have also considered the expansion $\ln(-\ln A + \alpha \ln N) = \ln \alpha + \ln(\ln N) + O[(\ln A)/(\alpha \ln N)]$ to zeroth order in $(\ln A)/(\alpha \ln N) \ll 1$, as we can check for $N \gtrsim 10^2$, $A \simeq 0.96$, and $\alpha \gtrsim 1/2$. Then, as we expect α to be similar to $1/2$ ($\alpha \simeq 0.56$ from the fitting of the 2D data in Fig. 2), we replace $\ln \alpha$ in Eq. (14) by the Taylor expansion $\ln \alpha \simeq \ln(1/2) + 2\alpha - 1$, and solve for α . We finally arrive at the following approximate scaling for the transition noise with N :

$$\eta_c^{2D} \simeq A N^{-\alpha}, \quad \text{with} \quad (15a)$$

$$\alpha(N) \simeq \frac{1}{2} + \frac{\ln \left[\frac{A}{B} \left(\frac{1}{2} \ln N \right)^{1/2} \right]}{\ln N - 1} \quad \text{or} \quad (15b)$$

$$\eta_c^{2D} \simeq 1.8(N \ln N)^{-1/2} \quad \text{for } N \gg 1, \quad (15c)$$

using $B \simeq 1.3$. In the inset of Fig. 2 we can see that the approximation from Eq. (15c) (bottom solid curve) reproduces very well the behavior of η_c^{2D} vs N from simulations (squares). The second term in the exponent $\alpha(N)$ [Eq. (15b)] leads to a very slow curvature in log-log scale with an effective exponent $\alpha \simeq 0.56$ in the shown range of N , which approaches very slowly the value $1/2$ as N increases. Finally, from Eq. (15c) we can see that the transition point η_c^{2D} vanishes in the $N \rightarrow \infty$ limit.

Summarizing the results of this section, the static version of the FVM in 1D and 2D lattices exhibits an order-disorder transition at zero noise in the thermodynamic limit.

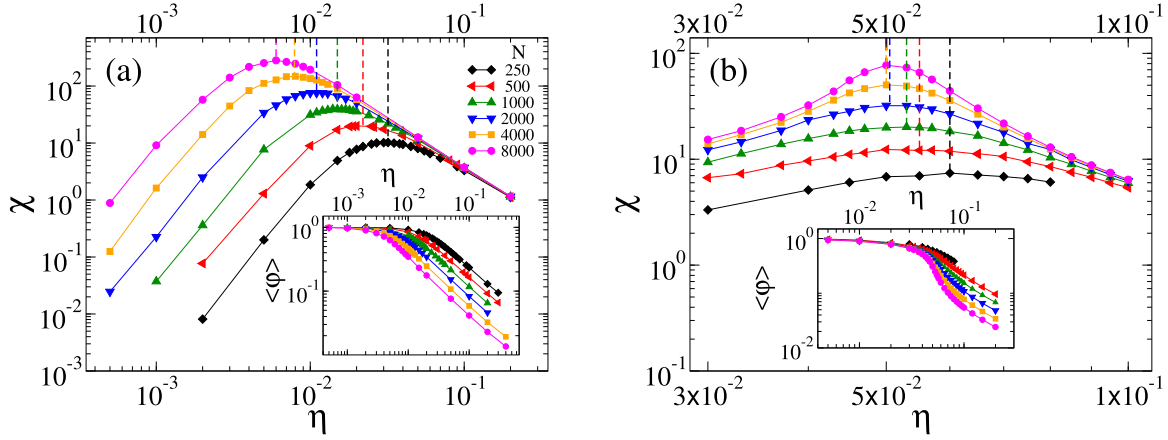


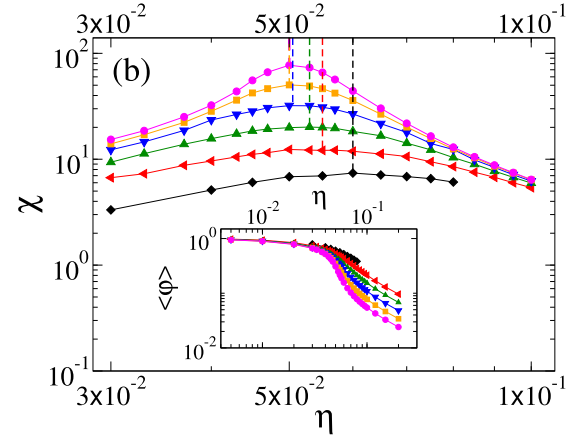
FIG. 5. Results of the dynamic version of the FVM in a 2D continuous space with particles' speed $v = 0.1$ (a) and $v = 1.0$ (b). The main panels show the susceptibility χ vs noise amplitude η for the system sizes indicated in the legend. The insets show the average of the order parameter $\langle\phi\rangle$ vs η . Vertical dashed lines indicate the estimated location of the transition noise η_c (maximum of χ).

V. DYNAMIC CASE $v > 0$ IN TWO DIMENSIONS

When particles are allowed to move over the space, their speed v becomes a relevant parameter that drastically changes the behavior of the system respect to the static case analyzed in Sec. IV, as we shall see below. Simulations were done on a 2D continuous space (square box) using the parallel dynamics defined in Sec. II; the standard update used in flocking dynamics [1]. As happens in MF, 1D, and 2D lattices, we expect to find similar results for a random update. We remark that interactions are local, that is, each particle can only interact with other particles that are less than a distance $R = 1$ apart, by copying the direction of one of them chosen at random.

In Fig. 5 we plot the susceptibility χ and the order parameter $\langle\phi\rangle$ (inset) vs noise amplitude η for speeds $v = 0.1$ [Fig. 5(a)] and $v = 1.0$ [Fig. 5(b)]. In principle, we observe a behavior similar to that of MF and the 1D and 2D static cases studied previously where $\langle\phi\rangle$ decays monotonically with η , and χ exhibits a maximum at a value η_c that decreases with N , as we can clearly see for $v = 0.1$. However, an inspection of the $v = 1.0$ plot reveals that η_c appears to decrease and saturate at a minimum value $\eta_c \simeq 0.05$ as N increases, unlike in MF and the static cases where η_c vanishes with N . Also, if we compare the level of order $\langle\phi\rangle$ and its fluctuations χ for the two speeds, we can see a larger order with smaller fluctuations for the largest speed $v = 1.0$, suggesting that the speed has an ordering effect.

To look at this in more detail, we plot in Fig. 6 the transition noise $\eta_c(v, N)$ vs the system size N for different speeds. Indeed, for a given speed $v \gtrsim 0.2$, we can see that η_c exhibits a decay similar to a power law for small values of N , and saturates at a minimum value $\eta_c(v, \infty) > 0$ for large N , which decreases as v decreases. We also plot for comparison the transition noise $\eta_c^{2D}(N)$ for the static case $v = 0$ in 2D lattices (empty circles). For the sake of clarity, the dashed line has been shifted in the y-axis to match the estimated asymptotic behavior of $\eta_c(v, N)$ in the zero speed limit $v \rightarrow 0$, as we do not expect $\eta_c^{2D}(N)$ and $\eta_c(0, N)$ to be exactly the same. This is because some macroscopic magnitudes of the dynamic model ($\langle\phi\rangle$, χ and η_c) depend on other variables besides v and N , such as the density of particles ρ .



The numerical results described above show that, in the thermodynamic limit, there is an order-disorder transition at a finite noise amplitude $\eta_c > 0$ that increases with the speed v . To study this transition in more detail, we investigate below the scaling behavior of η_c with the speed and the system size.

Since we have learned in Sec. IV that working with an effective noise $\hat{\eta}$ in 2D lattices leads to scalings with simple MF exponents, it seems reasonable to explore the data of Fig. 6 for an effective transition noise

$$\hat{\eta}_c(v, N) \equiv \eta_c(v, N) \sqrt{-\ln \eta_c(v, N)}, \quad (16)$$

which incorporates a correction factor $\sqrt{-\ln \eta_c}$ to the original noise η_c . The approximate power-law decay of η_c for small N and its saturation for large N [Fig. 6(a)] suggests that the scaling behavior of $\hat{\eta}_c(v, N)$ could be described by the following standard Family-Vicsek function with two independent exponents β and z [30]:

$$\hat{\eta}_c(v, N) \sim v^\beta f(v^z N), \quad (17)$$

where f is a scaling function with the asymptotic properties

$$f(x) \sim \begin{cases} x^{-\alpha} & \text{for } x \ll 1, \\ \text{constant} & \text{for } x \gg 1. \end{cases} \quad (18)$$

We can check that Eq. (17) exhibits the two limiting behaviors

$$\hat{\eta}_c(v, N \rightarrow \infty) \sim v^\beta \quad (19)$$

in the thermodynamic limit, and

$$\hat{\eta}_c(v \rightarrow 0, N) \sim N^{-\alpha} \quad (20)$$

in the zero speed limit, where the exponent α satisfies the relation

$$\beta = z\alpha. \quad (21)$$

By means of the scaling relation Eq. (17) we can collapse the data points of Fig. 6 into a single curve. For that, we first estimate the exponents β , α and z . From the plot $\hat{\eta}_c(v, \infty)$ vs v in the inset of Fig. 6 (squares) we find the best power-law fitting $C v^\beta$ (straight line), where $C = 0.095 \pm 0.01$ and $\beta = 1.01 \pm 0.02$. Then in the zero speed limit we assume that α takes the value $\alpha = \alpha^{2D} = 1/2$ of the 2D static case, and thus we obtain $z = 2.02 \pm 0.04$ from Eq. (21). Based on these

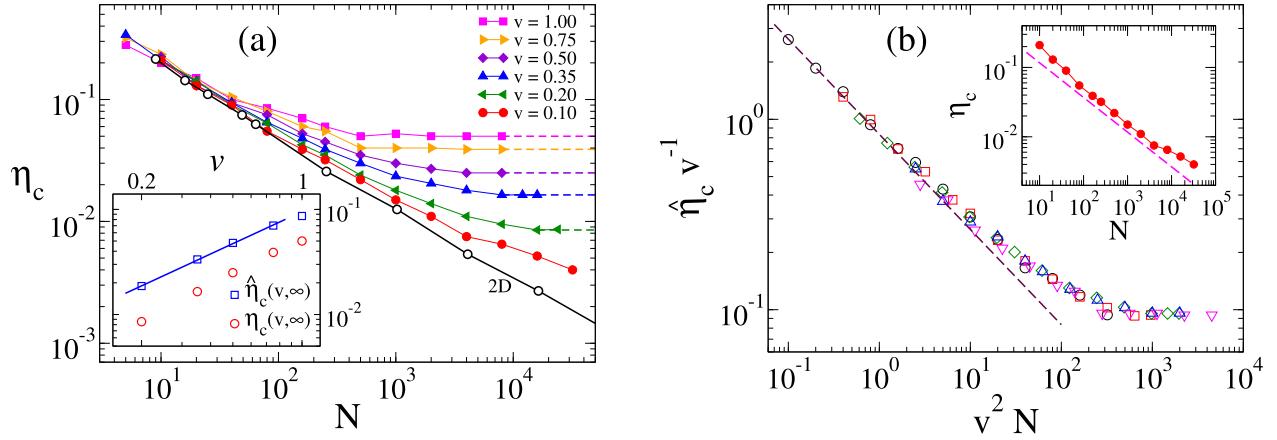


FIG. 6. (a) Transition noise η_c vs system size N for the speeds v indicated in the legend. The empty circles correspond to the 2D static case ($v = 0$) on square lattices. The horizontal dashed lines indicate the asymptotic values $\eta_c(v, \infty)$ for large N . Inset: Transition noise $\eta_c(v, \infty)$ vs v (circles) obtained from the main panel, and effective transition noise $\hat{\eta}_c(v, \infty)$ vs v (squares). The straight line is best power-law fit $C v^\beta$ of $\hat{\eta}_c(v, \infty)$ for $v \lesssim 0.75$, with resulting constant $C = 0.095 \pm 0.01$ and exponent 1.01 ± 0.02 . (b) Collapse of the curves for the different speeds of panel (a) by means of $\hat{\eta}_c(v, N)$. The exponents $z = 2$ and $\beta = 1$ in the x - and y -axis, respectively, correspond to the scaling Eq. (22). The dashed line with slope $-1/2$ indicates the power-law regime for $v^2 N \lesssim 2$. The inset shows η_c vs N for $v = 0.1$. The dashed line has slope $-1/2$.

exponents, we propose the following scaling for the effective transition noise:

$$\hat{\eta}_c(v, N) \sim v f(v^2 N), \quad (22)$$

with $f(x) \sim x^{-1/2}$ for $x \ll 1$ and $f(x) \sim \text{const}$ for $x \gg 1$. Figure 6(b) shows a good data collapse obtained with the scaling Eq. (22). Remarkably, this result required only the estimation of the best fitting exponent β of the $\hat{\eta}_c(v, \infty)$ vs v data, and assuming that the scaling of the transition noise with N in the zero speed limit is the same as that of the 2D static case.

The effective transition noise given by Eq. (22) scales linearly with the speed in the thermodynamic limit,

$$\hat{\eta}_c(v, \infty) \simeq C v, \quad (23)$$

where $C = 0.095$ is the best fitting constant for low speeds $v \lesssim 0.75$ [straight line in the inset of Fig. 6(a)]. An approximate power-law scaling $\eta_c(v, \infty) \simeq D v^\beta$ for the original noise can be obtained by following the same approach described in Sec. IV to obtain the scaling of η_c^{2D} with N [Eq. (15)]. For that, we start from the relation between $\hat{\eta}_c$ and η_c in logarithmic scale $\ln \hat{\eta}_c = \ln \eta_c + (1/2) \ln(-\ln \eta_c)$ and replace $\ln \hat{\eta}_c$ by $\ln C + \ln v$ [Eq. (23)] and $\ln \eta_c$ by $\ln D + \beta \ln v$. After rearranging terms and making the approximation $\ln(-\ln D - \beta \ln v) \simeq \ln \beta + \ln(-\ln v)$ to zeroth order in $(\ln D)/(\beta \ln v) < 1$ we arrive at

$$2(\beta - 1) \ln v - 2 \ln(C/D) + \ln(-\ln v) + \ln \beta = 0. \quad (24)$$

As we expect β to be similar to 1.0 [circles in the inset of Fig. 6(a)], we use the linear approximation $\ln \beta \simeq \beta - 1$ in Eq. (24) and solve for β . We finally obtain the following approximate expressions for the transition noise:

$$\eta_c(v, \infty) \simeq D v^\beta, \quad \text{with} \quad (25a)$$

$$\beta(v) \simeq 1 + \frac{\ln \left[\frac{C}{D} (-\ln v)^{-1/2} \right]}{\ln v + 1/2} \quad \text{or} \quad (25b)$$

$$\eta_c(v, \infty) \simeq C v (-\ln v)^{-1/2} \quad \text{for } v \ll 1. \quad (25c)$$

The second term in Eq. (25b) gives an effective exponent $\beta(v) \gtrsim 1$ that decreases and approaches the value 1 very slowly as v decreases. Equations (25) are valid only for low speeds due to the fact that the approximate expansion of the logarithm that we used in Eq. (24) assumes that $(\ln D)/(\beta \ln v) < 1$, which happens for $v \lesssim 0.08$. Unfortunately, the comparison of Eq. (25) with simulation results is not possible because to obtain the numerical value $\eta_c(v, \infty)$ for speeds $v < 0.2$ is extremely costly in terms of simulation running times.

Equation (22) also implies the scaling

$$\hat{\eta}_c(v, N) \sim N^{-1/2} \quad \text{for } v^2 N \ll 1, \quad (26)$$

which is confirmed in Fig. 6(b), where the collapsed data exhibit an approximate power-law decay with exponent $-1/2$ for $v^2 N \lesssim 2$, denoted by the dashed line. Finally, in the inset of Fig. 6(b) we compare the curve η_c vs N for the lowest speed $v = 0.1$ with the $N^{-1/2}$ scaling (dashed line). A good agreement is observed only at intermediate values of N , while for small or large sizes a deviation from the slope $-1/2$ becomes clear. We understand that the discrepancy for small N is due to the absence of the logarithmic correction $\sqrt{-\ln \eta_c}$ that becomes more relevant as η_c decreases, while for large N we expect that η_c reaches a saturation at a minimum value $\eta_c(0.1, \infty) > 0$. This asymptotic value of $\eta_c(0.1, N)$ is reached for system sizes outside the shown range and, in general, the approximate system size from where we start to see a plateau in η_c seems to diverge as v approaches zero [see Fig. 6(a)]. An insight into this can be given in terms of the crossover size N_{cross} that separates the two limiting behaviors of $\eta_c(v, N)$ for small and large N . For $N \ll N_{\text{cross}}$ the effective transition noise decays with N as $\hat{\eta}_c \sim N^{-1/2}$, while for $N \gg N_{\text{cross}}$ is $\hat{\eta}_c \sim v$. At the crossover size, these two limiting scalings should match, leading to $N_{\text{cross}} \sim v^{-2}$. This simple relation shows that, as v approaches zero, the crossover size diverges very fast, and so we need to run

simulations in very large systems to observe the asymptotic value of $\eta_c(v, N)$.

In summary, we showed in this section that the FVM in a 2D continuous space exhibits an order-disorder phase transition at a finite noise amplitude $\eta_c > 0$ that is proportional to the speed v of particles. For low speeds, η_c is linear in v with a logarithmic correction that leads to an effective power law with a v -dependent exponent slightly larger than 1. Thus, the transition at a finite noise $\eta_c > 0$ induced by particles' motion is in contrast with the zero-noise transition found in MF and the static version of the model in lattices.

VI. SUMMARY AND CONCLUSIONS

We studied a model for the flocking dynamics of self-propelled particles with pairwise copying interactions and noise. This model can be considered as a version of the noisy voter model with infinite number of angular states, which also incorporates the motion of particles over the space. We focused on the ordering properties of the system by exploring the order parameter φ that measures the global level of alignment of particles. We found that the system undergoes a transition as the noise amplitude η overcomes a threshold η_c , from an ordered phase for $\eta < \eta_c$ where a fraction of particles are aligned and thus $\varphi > 0$, to a disordered phase for $\eta > \eta_c$ characterized by each particle moving in a random direction, leading to $\varphi = 0$. We performed a numerical analysis to investigate how the speed of particles, the space and its dimension affect the order-disorder phase transition. We started by the simplest case of all-to-all interactions or infinite dimension or MF, followed by the static case of fixed particles on 1D and 2D square lattices, and ending with the dynamic case of particles moving on a bounded continuous 2D space. The transition point η_c was determined by the location of the peak of the susceptibility, which depends on the system size N . By doing suitable finite size scaling analysis we were able to infer the scaling behavior of the relevant magnitudes in the thermodynamic limit, including the transition noise.

In the MF case we showed that the transition noise vanishes with N as $\eta_c^{\text{MF}} \sim N^{-1/2}$, which is related to known analytical MF results of the MSVM. In the static case ($v = 0$) we found the scalings $\eta_c^{\text{1D}} \sim N^{-1}$ in one dimension and $\hat{\eta}_c^{\text{2D}} \sim N^{-1/2}$ in two dimensions, where $\hat{\eta}_c^{\text{2D}} = \eta_c^{\text{2D}} \sqrt{-\ln \eta_c^{\text{2D}}}$ is an effective noise amplitude. This effective noise with a logarithmic correction in η_c^{2D} was found by drawing an analogy between our FVM and the FGZ model for catalytic reactions with desorption probability p_d , and making the transformation $p_d \rightarrow \eta^2$. Our scaling results on MF and lattices are compatible with those predicted theoretically for the FGZ model, which is a version of the noisy two-state voter model.

We therefore conclude that, in MF and 1D and 2D static cases, the FVM displays an order-disorder transition at zero noise in the thermodynamic limit. This result means that any finite noise suppresses completely any level of order in the thermodynamic limit. That is, even a tiny amount of noise is enough to bring the system to complete disorder.

The behavior of the model in the dynamic case, where particles move at a finite speed $v > 0$ on a 2D box, is very different from that of the MF and static cases. We observed that, for a fixed density of particles $\rho = 0.5$ and a given

noise $\eta > 0$, increasing the speed leads to a larger value of φ with smaller fluctuations (smaller susceptibility χ), eventually inducing a stationary state of collective order for high enough speeds. We understand that this ordering effect produced by particles' motion is analogous to that found in Vicsek-type models, and, as a consequence, the system exhibits an ordered phase below a finite transition noise amplitude $\eta_c(v) > 0$ that depends on the speed. For low speeds, the behavior of the effective transition noise $\hat{\eta}_c = \eta_c \sqrt{-\ln \eta_c}$ with v and N is well described by a scaling function with two simple exponents. On the one hand, this leads to the scaling behavior $\hat{\eta}_c \sim N^{-1/2}$ for $v^2 N \ll 1$, which agrees with that of the 2D static case, and also with the theory developed for the saturation transition in the FGZ model [18,19]. On the other hand, the effective noise reaches an asymptotic value as N increases, which behaves as $\hat{\eta}_c \sim v$ in the $N \rightarrow \infty$ limit. This results in a transition noise with a superlinear dependence on the speed of the form $\eta_c \sim v(-\ln v)^{-1/2}$ for $v \ll 1$, in the thermodynamic limit. For the sake of comparison, it was recently found that in the Vicsek model the transition noise scales as $\eta_c \sim v^{0.45}$ in the low-density and low-speed regime [31]. We also note that the transition noise for a given speed and density $\rho = 0.5$ in the FVM is much smaller than that of the Vicsek model.

In summary, we found that the collective motion of self-propelled particles on a 2D space with noisy voter interactions exhibits an order-disorder transition at a finite noise amplitude η_c proportional to the speed of particles. This is a surprising result within the literature of the voter model, as it is known that adding an external noise to the copying dynamics of the model wipes up collective order in the thermodynamic limit, and in this article we showed that order can indeed be sustained by particles' motion.

It seems that the effect of motion is to correlate distant particles generating a state of global order, as happens in the Vicsek model. Thus, it might be interesting to study the correlations between particles' velocities and positions in order to understand the mechanisms that lead to flocking in the model. We also note that the MF approximation, which predicts a transition at zero noise, fails for the full version of the FVM with particles moving at a finite speed, showing the importance of taking into account the space and motion of particles in real-life situations, as happens, for instance, in the recent experiments with fish [6] described in Sec. I. It would be worthwhile to develop a mathematical description of the FVM that goes beyond MF and accounts for correlations between particles, which could correctly capture the ordering effect of motion. Finally, within the context of the experiments in [6], the results we obtained in the present article suggests that a group of fish could eventually reach an asymptotic polarized state when the group size increases, depending on the relation between the amplitude of the spontaneous directional change (noise) of fish and their speed.

ACKNOWLEDGMENTS

We acknowledge financial support from CONICET (PIP 11220150100039CO) and (PIP 0443/2014). We also acknowledge support from Agencia Nacional de Promoción Científica y Tecnológica (PICT-2015-3628) and (PICT 2016 Nro 201-0215).

- [1] T. Vicsek and A. Zafiris, *Phys. Rep.* **517**, 71 (2012).
- [2] M. C. Marchetti, J. F. Joanny, S. Ramaswamy, T. B. Liverpool, J. Prost, M. Rao, and R. A. Simha, *Rev. Mod. Phys.* **85**, 1143 (2013).
- [3] A. M. Menzel, *Phys. Rep.* **554**, 1 (2015).
- [4] T. Vicsek, A. Czirák, E. Ben-Jacob, I. Cohen, and O. Shochet, *Phys. Rev. Lett.* **75**, 1226 (1995).
- [5] J. Toner and Y. Tu, *Phys. Rev. Lett.* **75**, 4326 (1995).
- [6] J. Jhawar, R. G. Morris, U. R. Amith-kumar, M. Danny Raj, T. Rogers, H. Rajendran, and V. Guttal, *Nat. Phys.* **16**, 488 (2020).
- [7] G. Baglietto and F. Vazquez, *J. Stat. Mech.* (2018) 033403.
- [8] F. Vazquez, E. S. Loscar, and G. Baglietto, *Phys. Rev. E* **100**, 042301 (2019).
- [9] Y.-L. Chou and T. Ihle, *Phys. Rev. E* **91**, 022103 (2015).
- [10] A. Kirman, *Q. J. Econ.* **108**, 137 (1993).
- [11] B. L. Granovsky and N. Madras, *Stoch. Proc. Appl.* **55**, 23 (1995).
- [12] P. Clifford and A. Sudbury, *Biometrika* **60**, 581 (1973).
- [13] R. Holley and T. M. Liggett, *Ann. Probab.* **4**, 195 (1975).
- [14] M. Henkel, H. Hinrichsen, and S. Lübeck, *Non-Equilibrium Phase Transitions, Volume I: Absorbing Phase Transitions* (Springer, Bristol, UK, 2008).
- [15] K. Fichtorn, E. Gulari, and R. Ziff, *Chem. Eng. Sci.* **44**, 1411 (1989).
- [16] K. Fichtorn, E. Gulari, and R. Ziff, *Phys. Rev. Lett.* **63**, 1527 (1989).
- [17] D. Considine, S. Redner, and H. Takayasu, *Phys. Rev. Lett.* **63**, 2857 (1989).
- [18] E. Clement, P. Leroux-Hugon, and L. M. Sander, *Phys. Rev. Lett.* **67**, 1661 (1991).
- [19] E. Clement, P. Leroux-Hugon, and L. M. Sander, *J. Stat. Phys.* **65**, 925 (1991).
- [20] C. Flament, E. Clement, P. Leroux Hugon, and L. M. Sander, *Phys. A: Math. Gen.* **25**, L1311 (1992).
- [21] A. Carro, R. Toral, and M. San Miguel, *Sci. Rep.* **6**, 24775 (2016).
- [22] A. F. Peralta, A. Carro, M. S. Miguel, and R. Toral, *New J. Phys.* **20**, 103045 (2018).
- [23] A. F. Peralta, A. Carro, M. San Miguel, and R. Toral, *Chaos* **28**, 075516 (2018).
- [24] F. Herréras-Azcué and T. Galla, *Phys. Rev. E* **100**, 022304 (2019).
- [25] R. Martínez-García, C. López, and F. Vazquez, *Phys. Rev. E* **103**, 032406 (2021).
- [26] N. D. Mermin and H. Wagner, *Phys. Rev. Lett.* **17**, 1133 (1966).
- [27] R. A. Blythe and A. J. McKane, *J. Stat. Mech.* (2007) P07018.
- [28] M. Starnini, A. Baronchelli, and R. Pastor-Satorras, *J. Stat. Mech.* (2012) P10027.
- [29] W. Pickering and C. Lim, *Phys. Rev. E* **93**, 032318 (2016).
- [30] F. Family and T. Vicsek, *J. Phys. A: Math. Gen.* **18**, L75 (1985).
- [31] M. L. Rubio Puzo, A. De Virgiliis, and T. S. Grigera, *Phys. Rev. E* **99**, 052602 (2019).